Animal Models of Diabetic Complications Consortium
(**U01** HL087947)

Annual Report
(2007)

Modeling Diabetic Cardiomyopathy and Microangiopathy in the Mouse

University of Utah School of Medicine

Principal Investigator
Evan Dale Abel

Address: University of Utah School of Medicine, Division of Endocrinology Metabolism and Diabetes and Program in Human Molecular Biology and Genetics 15 North 2030 East, Bldg. 533, Room 4220, Salt Lake City, UT 84112

Phone: (801) 585-3635
E-mail: dale.abel@hmbg.utah.edu

Table of Contents

Animal Models of Diabetic Complications Consortium
(U01 HL087947)

Part A:

Principal Investigator's Summary

1. Program Accomplishments:

The University of Utah's participation in the Animal Models of Diabetes Complications Consortium proposed the generation of two mouse models. Model –1: *Modeling the role of insulin resistance, lipotoxicity and oxidative stress in the pathogenesis of diabetic cardiomyopathy* - ***CIRKO-ACS-sod2$^{+/-}$***
Model –2: *Modeling the role of impaired angiogenesis/arteriogenesis in the pathogenesis of microvascular complications of diabetes and to model the potential utility of increasing angiogenic potential as a strategy for preventing or reversing microvascular complications of diabetes.* – ***Inducible Netrin-Akita***

In addition we proposed hypothesis driven aims for both of these models.

MODEL 1: CIRKO-ACS-sod2$^{+/-}$.
The overall hypothesis that will be evaluated by this model is: *Diabetic cardiomyopathy is characterized by impaired myocardial insulin signaling, lipotoxicity and oxidative stress.* The proposed studies will test the following specific hypotheses:

1. The CIRKO-ACS-sod2$^{+/-}$ will meet the validation criteria for diabetic cardiomyopathy in terms of decreased contractile function, increased intramyocellular lipid and increased myocyte loss and fibrosis.
2. CIRKO-ACS-sod2$^{+/-}$ will exhibit increased rates of FA oxidation, decreased rates of glucose oxidation, increased MVO_2 and decreased cardiac efficiency.
3. The mechanism responsible for impaired myocardial function and substrate utilization in CIRKO-ACS-sod2$^{+/-}$ mice will be mitochondrial uncoupling on the basis of increased FA-mediated superoxide generation, leading to impaired mitochondrial energetics.
4. CIRKO-ACS-sod2$^{+/-}$ will develop rapid functional deterioration following hemodynamic stress such as pressure overload hypertrophy.

MODEL 2: Inducible-Netrin-Akita (*Tam-b-actinCRE.ROSA26* $^{netrin1/lacZ}$*.ins2*$^{+/C96Y}$).

The overall hypothesis that will be tested in this model is: *Impaired adaptive angiogenesis and arteriogenesis contributes to impaired myocardial remodeling following coronary ischemia, and to increased limb loss following femoral artery occlusion in diabetes.* These studies will utilize the inducible-netrin-akita mouse and take advantage of our ability to upregulate netrin expression in a temporal fashion by inducible activation of cre-recombinase following treatment of mice with tamoxifen. If inducible cardiomyocyte-restricted Cre-Netrin Akita mice are also developed, we can additionally determine if this approach will hold true in an organ-restricted manner as well. The studies proposed in this aim will initially determine the fidelity of the temporal (tamoxifen-inducible) gene expression system in inducible-netrin-akita mice. Based on preliminary data that we have obtained with the tamoxifen-regulated MHC Cre mouse (MCM-MHC) we are confident that we will be able to increase netrin expression in cardiomyocytes of netrin-Akita mice, and deem it likely that more widespread netrin activation will be obtained with the inducible beta-actin driven tamoxifen cre transgenic (*Tam-b-actinCRE.ROSA26* $^{netrin1/lacZ}$*.ins2*$^{+/C96Y}$).

The following hypotheses will be tested:

1. Tamoxifen treatment of *Tam-b-actinCRE.ROSA26* $^{netrin1/lacZ}$*.ins2*$^{+/C96Y}$ mice will increase netrin1 expression ubiquitously, including cardiomyocytes and skeletal muscle. Tamoxifen treatment of *MCM-MHC.ROSA26* $^{netrin1/lacZ}$*.ins2*$^{+/C96Y}$ (if generated) will increase netrin expression in cardiomyocytes only.
2. Diabetic animals will exhibit accelerated myocardial remodeling following coronary artery occlusion and relative to control animals and the promotion of angiogenesis and arteriogenesis by netrin1 will reverse this phenotype
3. Diabetic animals will exhibit reduced recovery of hind-limb perfusion following femoral artery ligation relative to non-diabetic animals and the promotion of angiogenesis and arteriogenesis by netrin1 will reverse this phenotype

Recent Progress and Major Accomplishments

Summary of milestone targets that were submitted in October 2006

1. To determine myocardial substrate metabolism in the heart of young ACS mice.
2. To determine the mechanisms responsible for the changes in mitochondrial function and morphology in ACS transgenic mice.
3. To determine insulin sensitivity in the hearts of ACS mice.
4. To determine the mechanisms responsible for increased ROS generation and mitochondrial uncoupling in the hearts of db/db mice.

Accomplishments related to October 2006 goals

Studies in MHC-ACS Mice: We have conducted extensive additional characterization of the cardiac and metabolic phenotypes of ACS transgenic mice. We observed that they developed age-related cardiac hypertrophy (Figure 1), but had remarkably normal LV function in vivo when evaluated by echocardiography (Figure 2). However, in isolated perfused hearts clear evidence for contractile dysfunction was evident as early as 8-weeks (Figure 3). Contrary to our original hypothesis ACS transgenic mice did not show increased rates of FA oxidation in isolated perfused heart preparations from 8 or 24-week-old mice (Figure 4). However there was increased accumulation of triglycerides and potentially toxic lipid-derived metabolites such as ceramide and diacyl glycerol (Figure 5). ACS mice developed age-related mitochondrial dysfunction that was evident in 12-week-old mice as mitochondrial uncoupling (reduced ATP/O ratios) followed by an age-related decline in mitochondrial oxygen consumption (Figure 6). ROS production in mitochondria from ACS and CIRKO-ACS mice was increased and this appeared to derive primarily from Complex I of the mitochondrial respiratory chain. This conclusion is based on the observation that inhibition of complex I activity with rotenone completely abrogated ROS production (Figure 7) and direct assay of complex I activity following blue-native gel electrophoresis, which revealed elevated complex I activity (Figure 8). Despite the increase in ROS production, the activity levels of the ROS sensitive Aconitase was not reduced, implying that ROS defense mechanisms were activated in the hearts of ACS mice (Figure 9). These data therefore provide additional justification for limiting sod2 expression by crossing ACS mice with sod2$^{+/-}$ mice. ACS mice develop dramatic changes in mitochondrial morphology that are characterized by mitochondrial proliferation (increased mitochondrial number and mitochondrial volume density), and a reduction in mitochondrial size (Figure 10). These changes are not associated with activation of PGC-1α or PPAR-α regulated pathways (Figure 11), indicating the existing of underlying pathogenic mechanisms that might be distinct from, or develop in parallel with the potential role of PGC-1α and PPAR-α activation that occurs in models of obesity and diabetes such as *ob/ob* and *db/db* mice. We have not yet characterized insulin sensitivity in the hearts of ACS mice. We are currently backcrossing the ACS and CIRKO mice to the c57BL6/J background and are currently on the fourth generation.

Mechanisms responsible for increased ROS generation in the hearts of db/db mice: We demonstrated that db/db mice develop mitochondrial dysfunction due in part to a reduction in mitochondrial oxidative phosphorylation capacity. In addition db/db mitochondria became uncoupled

in the presence of increased fatty acids, which further decreased mitochondrial energetics. One mechanism for the FA-mediated mitochondrial uncoupling was an increase in ROS generation from Complex I and Complex III. A mechanism for increased ROS production was a mismatch between beta-oxidation and the delivery of reducing equivalents to the respiratory chain (which were both increased) and a reduction in the capacity of the respiratory chain to completely oxidize these reducing equivalents. The results of these studies were recently published in the Journal Diabetes.

Figure 1

ACS mice may develop mild hypertrophy

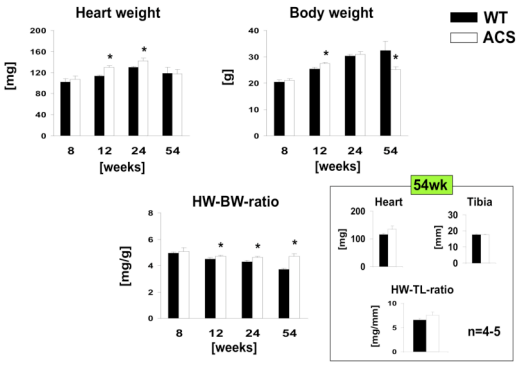

Figure 2

No signs of contractile dysfunction in ACS mice *in vivo*

	8 wk		24 wk		54 wk	
	WT	ACS	WT	ACS	WT	ACS
LVDd [cm]	0.37 ± 0.01	0.38 ± 0.01	0.40 ± 0.03	0.40 ± 0.02	0.40 ± 0.01	0.41 ± 0.01
LVDs [cm]	0.23 ± 0.01	0.25 ± 0.02	0.26 ± 0.03	0.25 ± 0.02	0.30 ± 0.01	0.30 ± 0.01
LVPWd [cm]	0.09 ± 0.01	0.08 ± 0.01	0.10 ± 0.01	0.09 ± 0.01	0.09 ± 0.01	0.08 ± 0.01
FS [%]	38.6 ± 2.4	35.3 ± 2.9	36.8 ± 4.2	38.4 ± 3.4	27.1 ± 2.4	27.6 ± 0.7
EF	0.78 ± 0.02	0.72 ± 0.04	0.74 ± 0.05	0.76 ± 0.04	0.60 ± 0.04	0.61 ± 0.01
CO [ml/min]	-	-	15.7 ± 1.2	13.4 ± 1.2	-	-

Figure 3

ACS mice develop contractile dysfunction *in vitro*

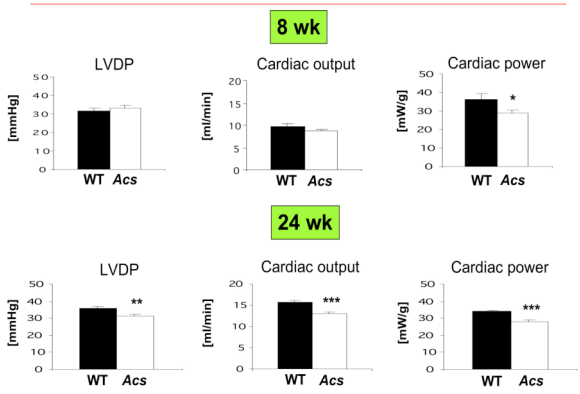

Figure 4

Reduced palmitate oxidation in ACS mice

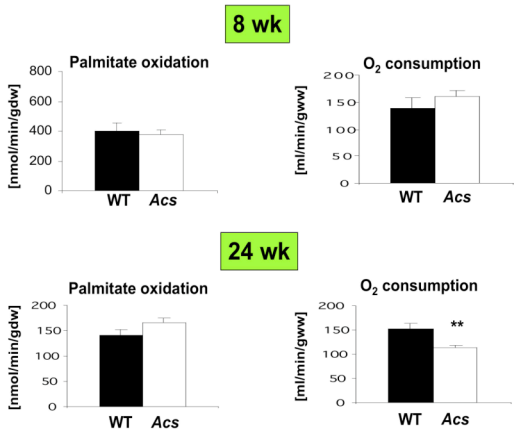

Figure 5: Intracellular triglycerides (L–panel) and Ceramide and Diacyl Glycerol levels (R-panel)

Intracellular triglyceride content

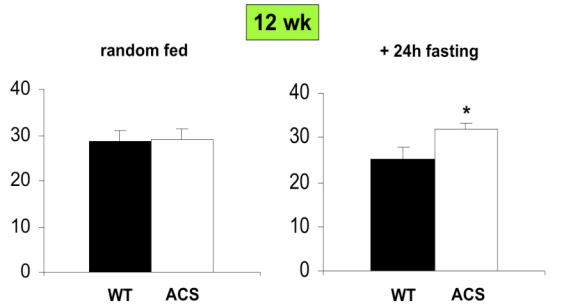

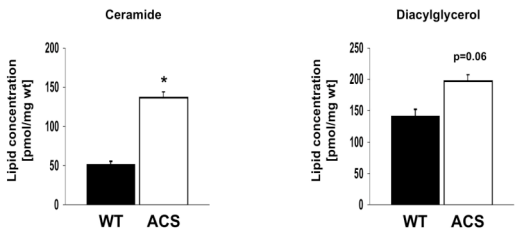

Figure 6

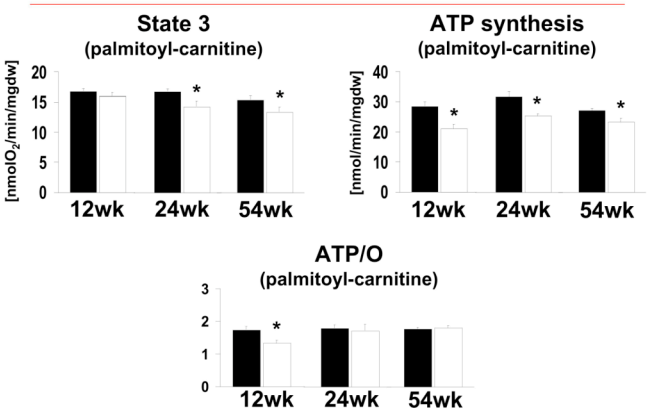

Figure 7

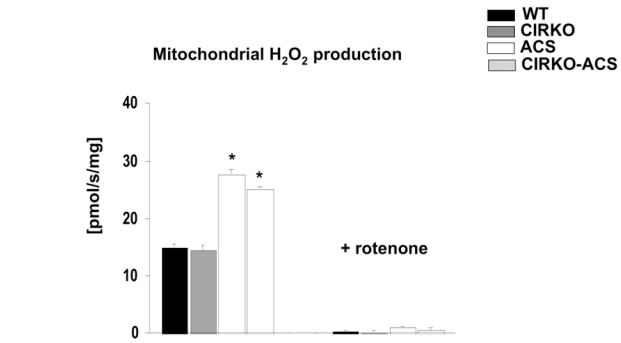

Figure 8

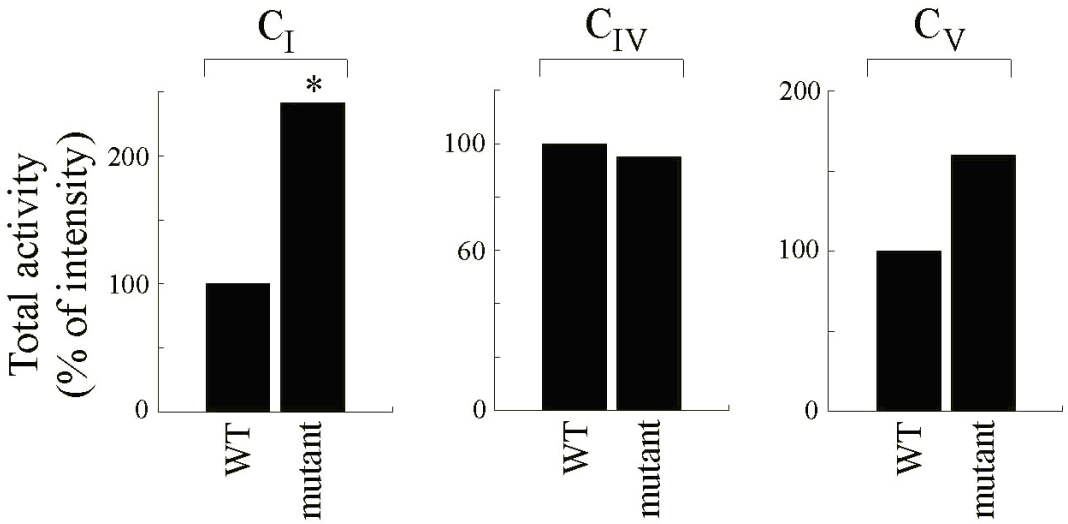

Figure 9

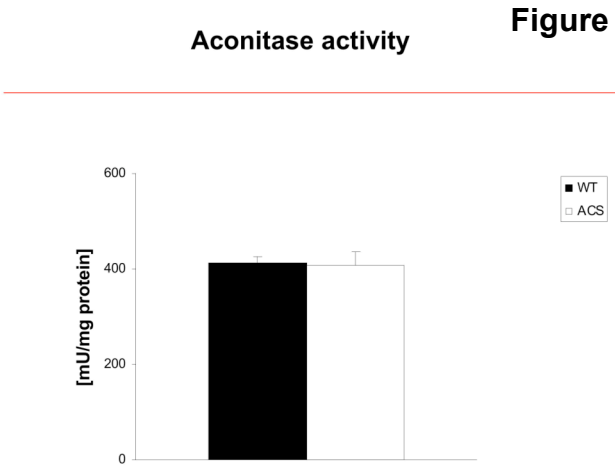

Figure 10

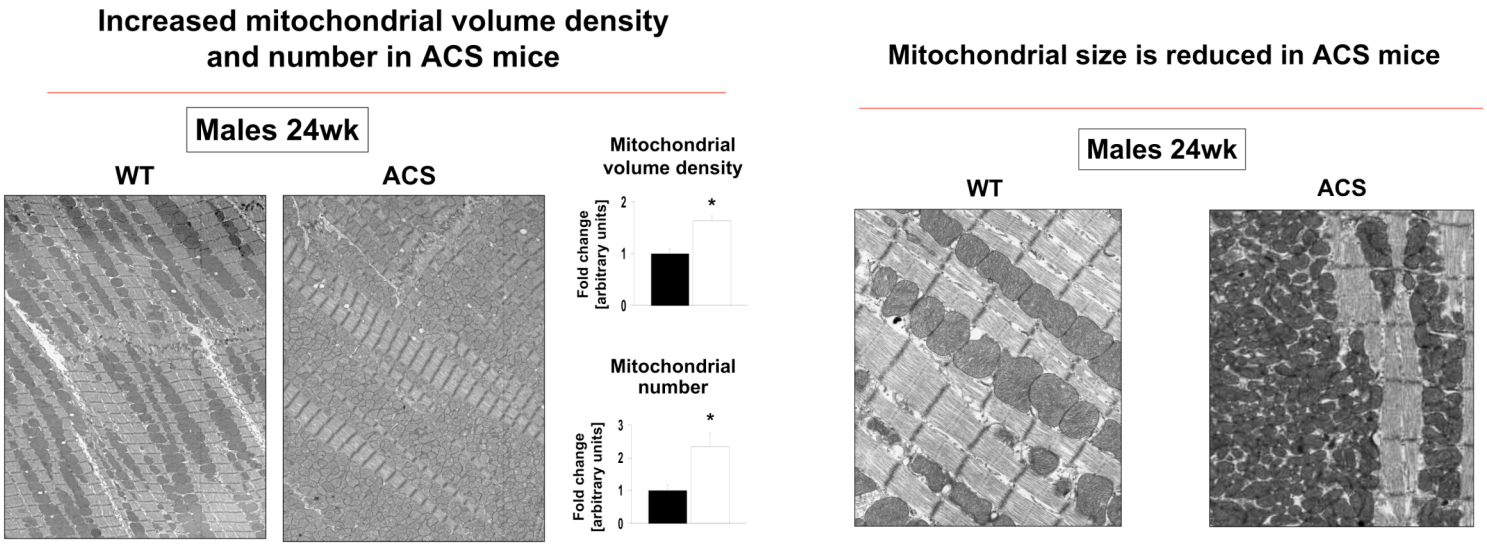

Figure 11

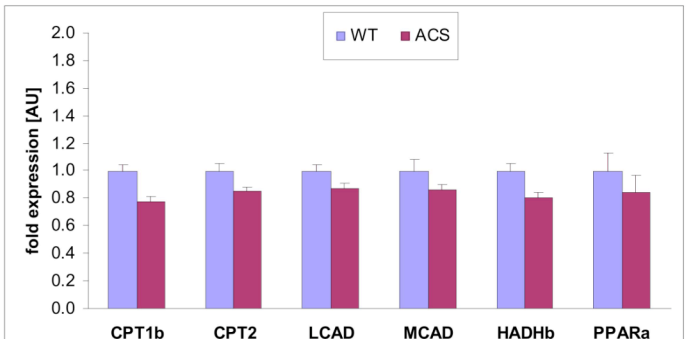

FAO Genes

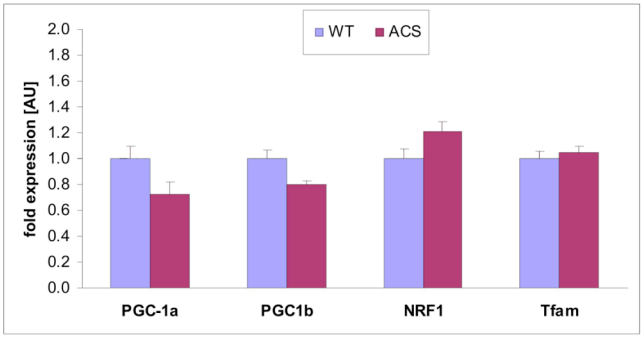

Mitochondrial Biogenesis Genes

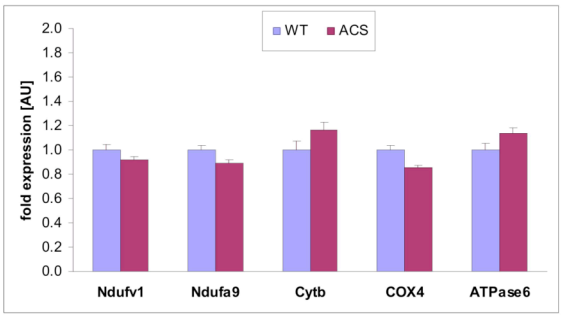

OXPHOS Genes

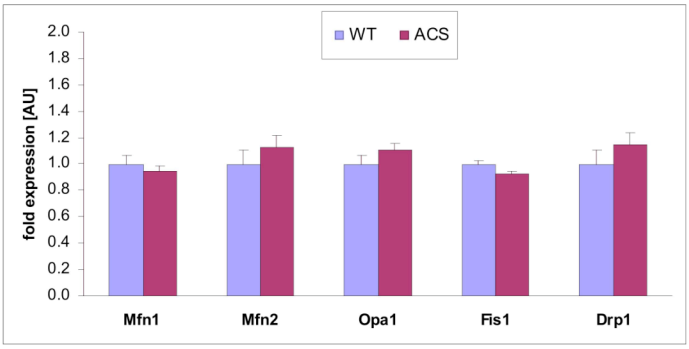

Mitochondrial Fusion and Fission Genes

Additional Accomplishments

Characterization of the cardiac phenotype of Akita mice:

The Akita mouse has emerged as an important platform within the AMDCC for modeling complications of type 1 diabetes after the introduction of a variety of genetic modifications. Moreover it will be the diabetic background upon which the inducible netrin-1 transgene will ultimately be placed. In the first round of the AMDCC, we conducted extensive characterization of the cardiac phenotype of models of type 2 diabetes. We felt that it was important to conduct a similarly detailed analysis of the cardiac phenotype of Akita mice. As expected, Akita mice were hyperglycemic and had increased serum concentrations of fatty acids and triglycerides (Figure 12). In contrast to models of type 2 diabetes, Akita mice do not spontaneously develop cardiac hypertrophy (Figure 13). Resting cardiac function was normal across a wide age-range (Figure 14), but the inotropic response to adrenergic stimulation (isoproterenol) was impaired (specifically a reduction in cardiac output), despite similar degrees of cardiac hypertrophy (Figure 15). Isolated hearts from Akita mice exhibit decreased LV developed pressure and an impaired inotropic response to insulin (Figure 16). Myocardial substrate metabolism was characterized by increased rates of FA oxidation and decreased rates of glucose oxidation, but in contrast to type 2 diabetes models, substrate metabolism was responsive to insulin (Figure 17). Akita mice developed mitochondrial dysfunction as evidenced by reduced rates of mitochondrial oxygen consumption, and reduced ATP production with glutamate and pyruvate substrates (Figure 18). In contrast to type 2 diabetes models such as the db/db mouse, Akita hearts did not show evidence of oxidative stress. Mitochondrial H_2O_2 production rates were actually reduced, ROS levels measured by DCF fluorescence were normal and there was no reduction in the levels of aconitase (Figure 19). Mitochondrial volume density was increased, but not mitochondrial number, implying an increase in mitochondrial size (Figure 20). At the level of gene expression there was a coordinate reduction of the expression of genes involved in mitochondrial OXPHOS and myocardial calcium handling but there was increased expression of PPAR-α regulated genes (Figure 21). Taken together these data highlight some important similarities (substrate metabolism and mitochondrial dysfunction) and important differences (absence of cardiac hypertrophy and oxidative stress and normal insulin sensitivity) between type 1 Akita mouse hearts and those of type 2 diabetic models such as ob/ob and db/db mice.

Figure 12

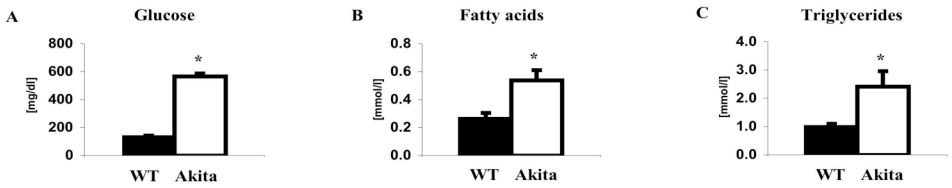

Figure 13

Table 1: Heart weight (HW), body weight, tibia length (TL), and HW-TL-ratio of 10, 24, and 54 week-old WT and Akita mice.

	Body weight	Heart weight	Tibia length	HW-TL-ratio
WT 10wk (6)	24.0 ± 0.8	111.3 ± 4.8	16.8 ± 0.2	6.6 ± 0.3
Akita 10wk (8)	22.4 ± 0.5	105.1 ± 2.2	16.5 ± 0.1	6.4 ± 0.1
WT 24wk (8)	27.9 ± 0.9	112.1 ± 2.3	17.4 ± 0.1	6.4 ± 0.1
Akita 24wk (6)	24.4 ± 0.4 Ψ	102.5 ± 2.2 *	17.1 ± 0.2	6.0 ± 0.1 *
WT 54wk (6)	31.5 ± 0.8	141.8 ± 4.2	17.7 ± 0.1	8.0 ± 0.2
Akita 54wk (3)	24.9 ± 0.4 Ψ	114.8 ± 1.0 Ψ	17.7 ± 0.2	6.5 ± 0.1 Ψ

* p<0.05, Ψ p<0.01 vs. WT

Figure 14

Table 2: Echocardiography of WT and Akita mice at 20 and 36 weeks of age.

	LVDd [cm]	LVDs [cm]	IVSd [cm]	LVPWd [cm]	FS [%]	EF	CO
WT 20wk (9)	0.38 ± 0.01	0.24 ± 0.01	0.08 ± 0.01	0.08 ± 0.01	38.6 ± 2.4	0.76 ± 0.03	13.0 ± 0.4
Akita 20wk (7)	0.38 ± 0.01	0.23 ± 0.01	0.08 ± 0.01	0.08 ± 0.01	38.7 ± 2.4	0.76 ± 0.03	12.9 ± 0.4
WT 36wk (6)	0.36 ± 0.02	0.22 ± 0.01	0.11 ± 0.01	0.10 ± 0.01	39.6 ± 1.2	0.78 ± 0.01	13.4 ± 0.8
Akita 36wk (5)	0.36 ± 0.01	0.22 ± 0.02	0.11 ± 0.01	0.11 ± 0.01	39.7 ± 2.7	0.78 ± 0.03	11.7 ± 0.8

LVDd, Left ventricular cavity diameter at diastole; LVDs, Left ventricular cavity diameter at systole; IVSd, Interventricular septum diameter at diastole; LVPWd, Left ventricular posterior wall thickness at diastole; FS, Fractional shortening; EF, Ejection fraction; CO, Cardiac output.

Figure 15

Table 3: Echocardiography of 10 week-old WT and Akita mice without treatment or treated with 17mg/kg/d Isoproterenol for 5 days (n=3).

	WT	WT + Isoproterenol	Akita	Akita + Isoproterenol
CO	10.3 ± 0.9	17.7 ± 1.5 Ψ	7.9 ± 0.3	8.7 ± 2.4 θ
EF	67.0 ± 2.6	81.0 ± 6.2	66.7 ± 2.0	72.0 ± 7.0
FS	31.3 ± 1.9	39.3 ± 3.8	29.0 ± 1.5	35.7 ± 5.5
HR	378 ± 17	599 ± 35 Ψ	360 ± 16	509 ± 27 Ψ θ
IVSd	0.087 ± 0.003	0.130 ± 0.012 Ψ	0.097 ± 0.012	0.107 ± 0.009
LVDd	0.377 ± 0.007	0.310 ± 0.015 Ψ	0.370 ± 0.012	0.327 ± 0.015 Ψ
LVDs	0.260 ± 0.006	0.187 ± 0.029 Ψ	0.260 ± 0.010	0.210 ± 0.015 Ψ
LVPWd	0.083 ± 0.003	0.123 ± 0.020 Ψ	0.087 ± 0.007	0.107 ± 0.007

CO, Cardiac output; EF, Ejection fraction; FS, Fractional shortening; HR, Heart rate; IVSd, Interventricular septum diameter at diastole; LVDd, Left ventricular cavity diameter at diastole; LVDs, Left ventricular cavity diameter at systole; LVPWd, Left ventricular posterior wall thickness at diastole. Ψ p<0.05 vs. without Isoproterenol, θ p<0.05 vs. WT + Isoproterenol

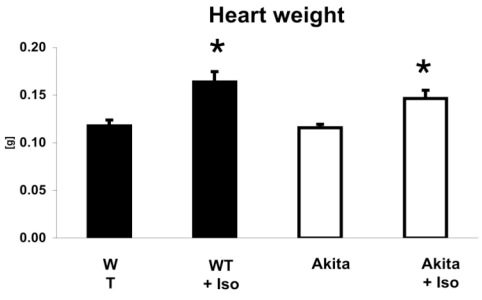

out Iso

Figure 16

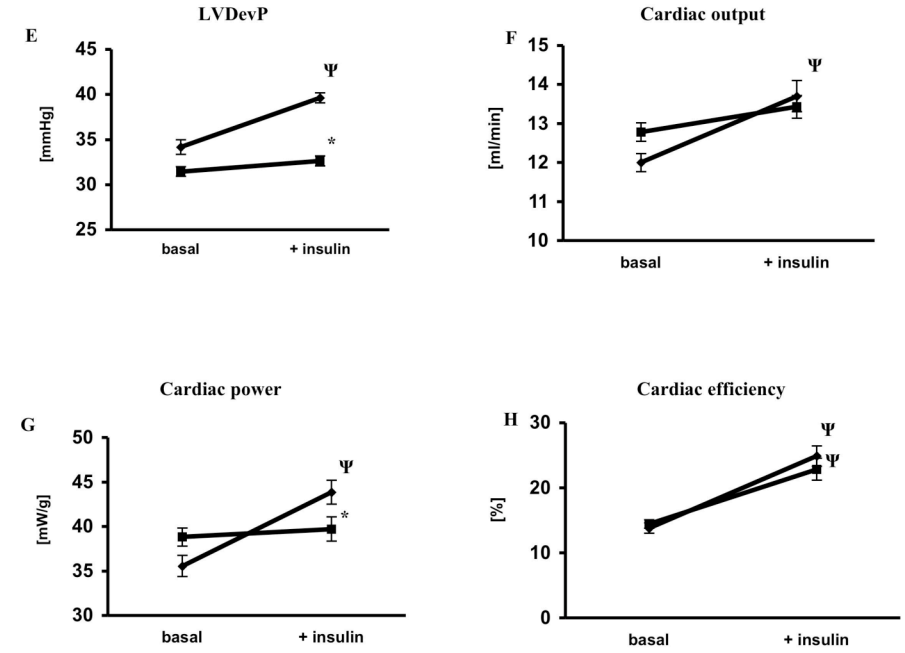

Ψ p<0.05 vs. without Insulin
*** p<0.05 vs. WT**

Figure 17

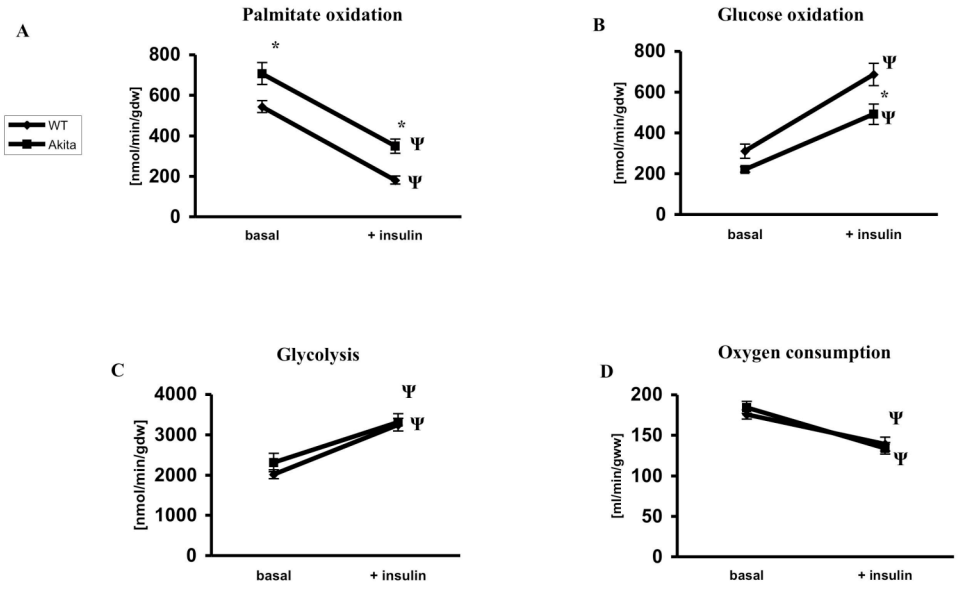

Ψ p<0.05 vs. without Insulin
*** p<0.05 vs. WT**

Figure 18

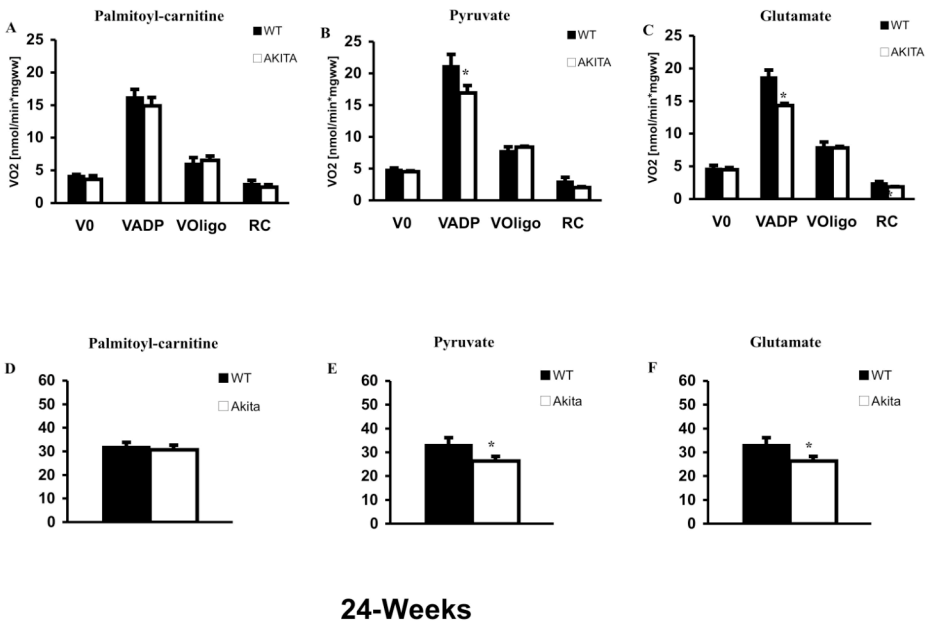

Figure 19

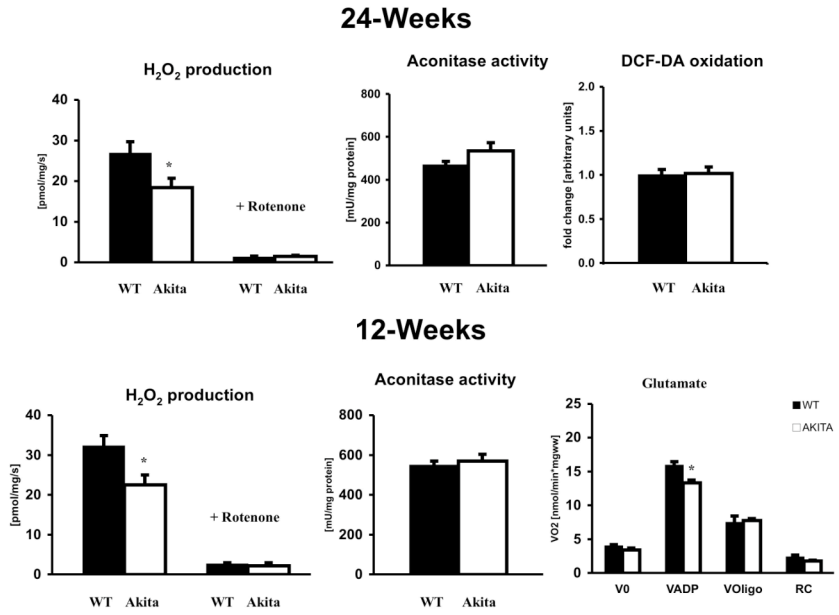

Figure 20

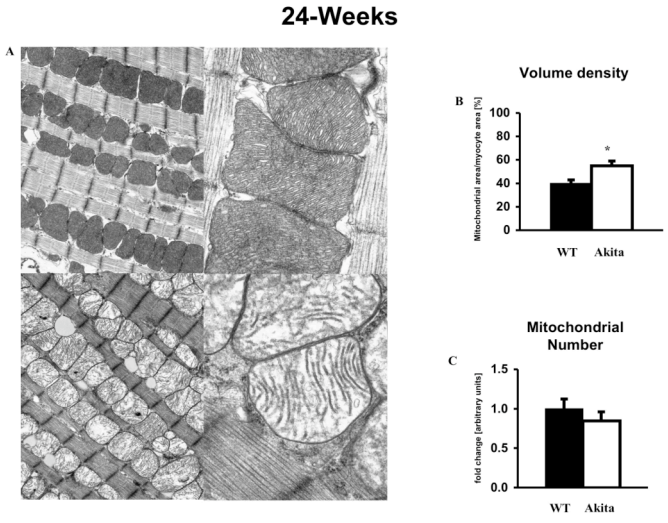

Figure 21

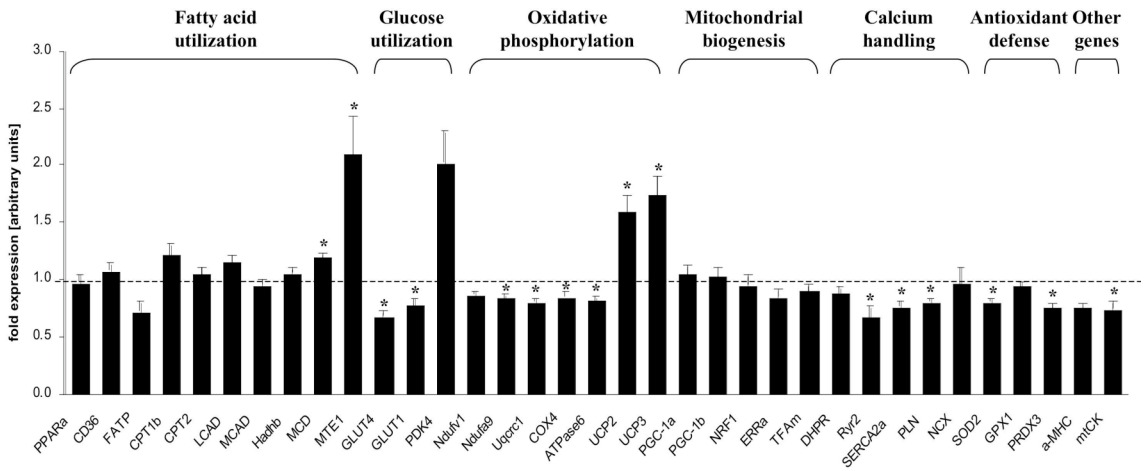

Establishment of the hind limb ischemia technique:

An important goal of our studies is a determination of the potential therapeutic role of netrin-1 (an angiogenic peptide) in reversing hind limb ischemia in mouse models of diabetes. We therefore developed the femoral artery ligation technique and have become trained in the laser Doppler technique for measuring hind limb blood flow recovery. Results from a series of C57BLKS controls and db/db mice are shown in Figures 22 and 23. As illustrated control animals develop significant restoration of hind limb blood flow as early as 2-weeks post femoral artery ligation and this recovery is completely absent in hind limbs of db/db mice.

Generation of Inducible-Netrin-Akita (Tam-b-actinCRE.ROSA26 $^{netrin1/lacZ}$*.ins2*$^{+/C96Y}$*).*

Prior to establishing the mechanism to send DNA or ES cell clones to the Jackson Laboratory as negotiated by the consortium, we submitted a gene-targeting construct containing a Netrin 1/lacZ cassette that will be knocked into the ROSA-26 locus to the local transgenic facility. We therefore have elected to wait to determine the outcome of this gene targeting experiment instead of sending the construct to Jackson Laboratories, as this would represent a duplication of effort. Two independent injections were performed. The first round produced two strong chimeras. These mice have been breeding but we have not seen germline transmission as yet. A second electroporation was performed which yielded additional ES cells, which yielded four positive lines, all of which were injected into blastocysts. There are ten high percentage chimeras for ES Cell # 297 and four for ES cell # 268. Pups have been generated from ES cell # 419 and # 423 but they are too young to determine the degree of chimerism at the present time. There are nine pups for 419 and 16 pups for 423. So we are cautiously optimistic that these chimeras will transmit to the germline. The first group of chimeras should be ready to go into breeding cages the third week in July. Once a suitable founder is identified, then mice will be sent to the Jackson Laboratory to be backcrossed to the C56BL6 strain and ultimately with the tamoxifen-inducible beta-actin Cre mouse.

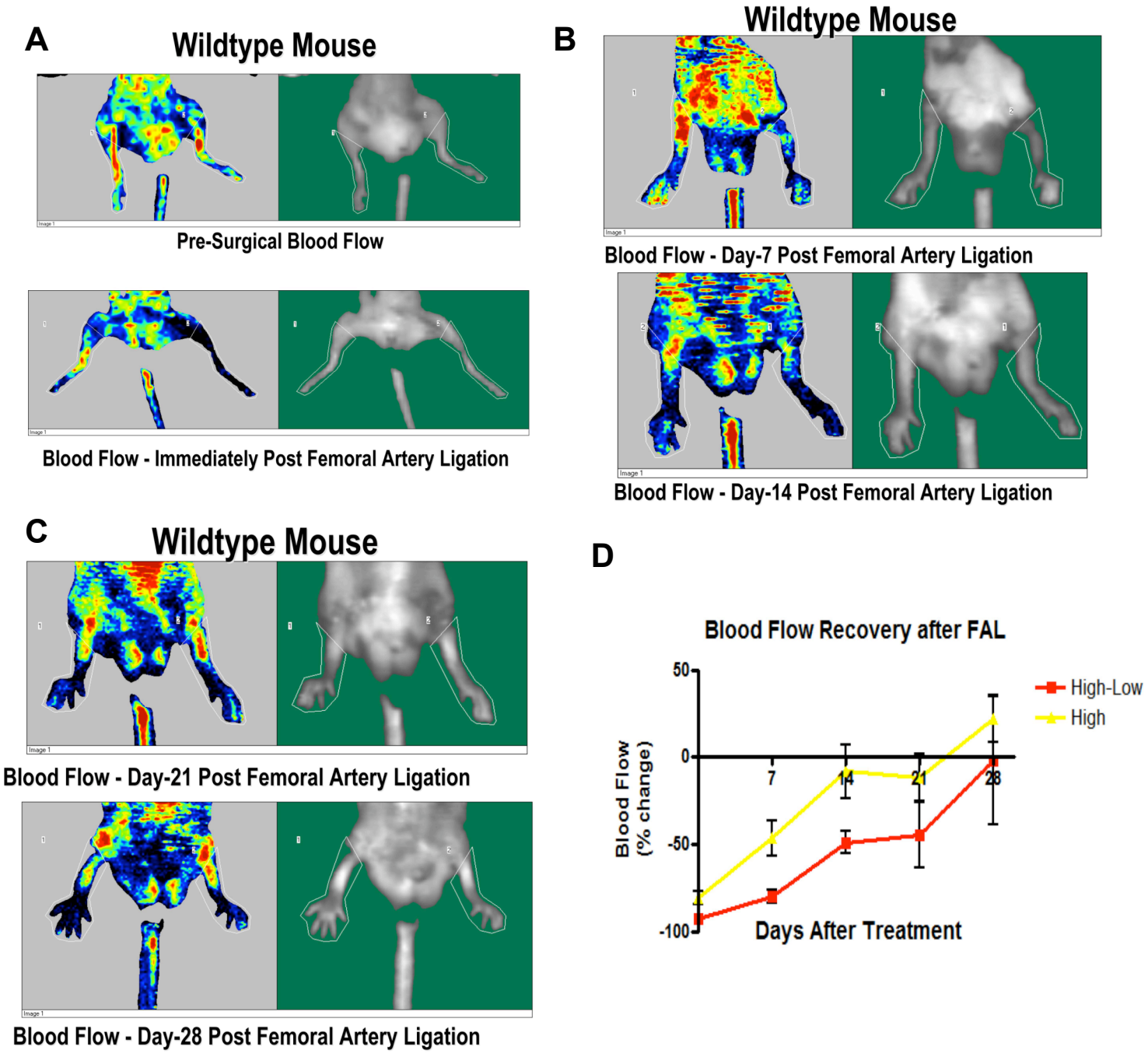

Figure 22: Blood Flow Recovery Following Femoral Artery Ligation in Control C57BL6 mice. Panels A-C are representative Doppler images of hind limb blood flow before and after ligation of the L Femoral Artery at the time points as shown. Panel D shows mean blood flow recovery in a cohort of wildtype mice following ligation of the femoral artery proximal to the deep femoral branch artery (high, n=6) or after dissection of an arterial segment from the deep femoral artery to the saphenous branch (high-low, n=5). Note, normalization of hind limb blood flow after 28-days.

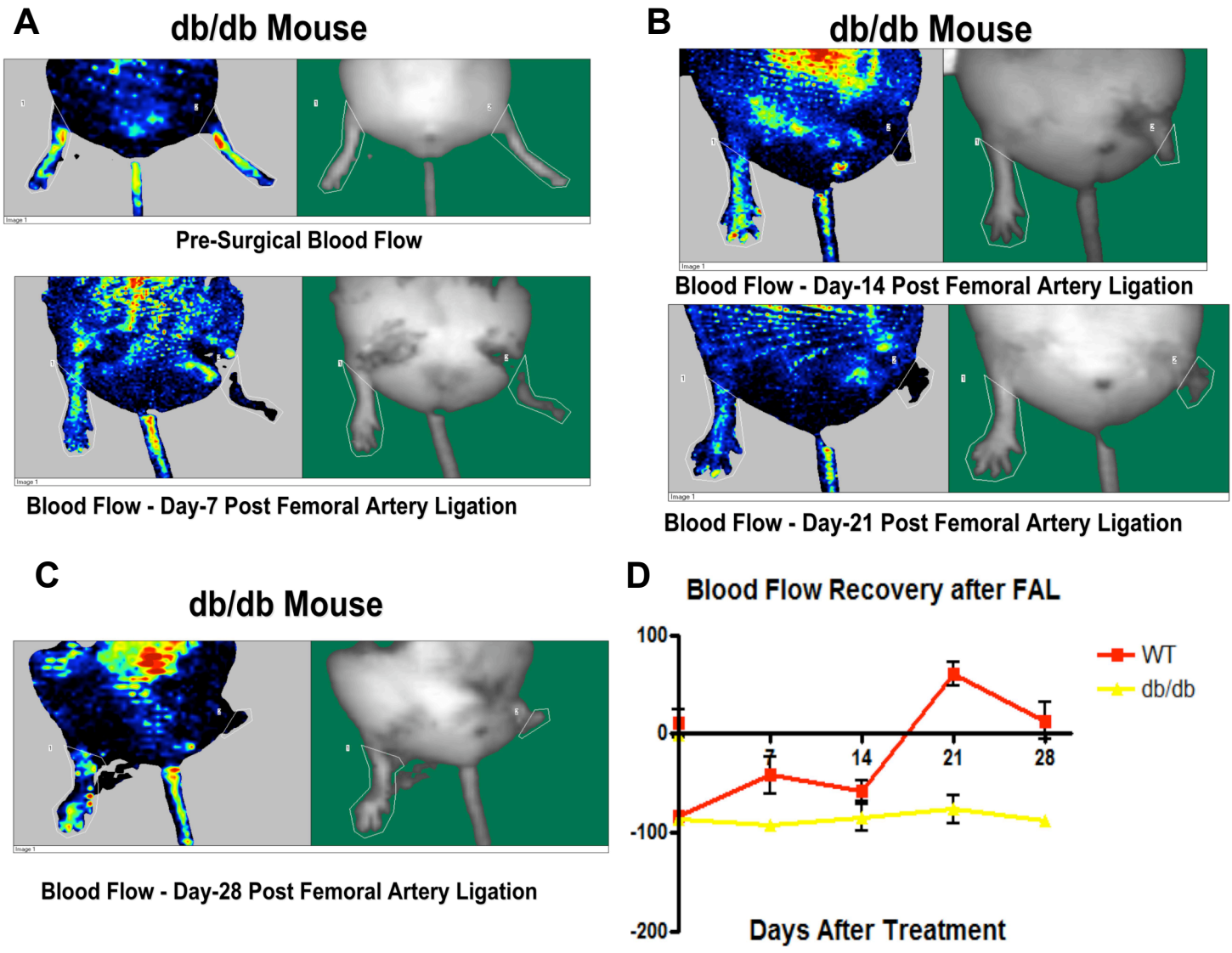

Figure 23: Blood Flow Recovery Following Femoral Artery Ligation in Diabetic *db/db* mice. Panels A-C are representative Doppler images of hind limb blood flow before and after ligation of the L Femoral Artery at the time points as shown. Panel D shows mean blood flow recovery in a cohort of 4 wildtype and 5 *db/db* mice for 28-days following femoral artery ligation. Note that whereas there is normalization of hind limb blood flow after 21-days in controls there is no revascularization in hind limbs of *db/db* animals.

Plans for the Upcoming Year

1. Complete the backcross MHC-ACS and CIRKO-ACS mice to the C57BL6 background.
2. Introduce sod2 heterozygous allele into the CIRKO-ACS mice on the C57BL6 background
3. Screen offspring of ROSA26 $^{netrin1/lacZ}$ for germline transmission and transfer mice to Jackson Laboratories for backcrossing into the Akita and Tamoxifen-inducible Cre lines.

Preliminary Milestones for 2009 and Beyond

1. Phenotypically characterize The CIRKO-ACS-sod2$^{+/-}$ as outlined in the specific aims.
2. Complete the generation of Tam-b-actinCRE.ROSA26 $^{netrin1/lacZ}$.ins2$^{+/C96Y}$ and phenotypically characterize as outlined in the specific aims.

2. Collaboration:

Within AMDCC

We have an active collaboration with Ira Goldberg, where we are characterizing substrate metabolism in the hearts of a mouse model of lipotoxic cardiomyopathy (mice with cardiomyocyte overexpression of a GPI-anchored lipoprotein lipase).

We transferred alpha- MHC Cre mice for the purpose of generating cardiomyocyte – restricted KO of type 1 angiotensin receptors.

With Jax

None as yet. We hope to send ROSA26 $^{netrin1/lacZ}$ mice once we verify germline transmission.

With the MMPCs

We have been working with Craig Molloy at the UTSW MMPC to develop heart perfusions that use both ^{13}-C isotopomers, as well as ^{3}-H and ^{14}-C tracers to determine myocardial metabolism in isolated working mouse hearts. The goal of these studies is to compare tracer isotope and NMR – based methods, which provide complementary data on cardiac metabolic substrate utilization.

With other non-AMDCC PIs

Cardiac and mitochondrial phenotyping in mice with myocardial expression of a dominant-negative clock transgene (Martin E. Young, Baylor University)

Determining the role of insulin resistance in the potentially protective cardiac effects of isocaloric diets, which are rich in saturated fatty acids when given to mice with pressure overload hypertrophy. This hypothesis is being tested by William Stanley at the University of Maryland to whom we have sent mice with cardiomyocyte-restricted KO of insulin receptors (CIRKO).

Characterization of the response of PGC-1β deficient hearts to pressure overload hypertrophy (in collaboration with Antonio Vidal Puig at the University of Cambridge).

3. Address previous EAC comments:

NOT APPLICABLE THIS YEAR

4. Publications:

Original Reports

1. Augustus AS, Buchanan J, Park TS, Hirata K, Noh HL, Sun J, Homma S, D'armiento J, **Abel ED**, Goldberg IJ. Loss of lipoprotein lipase-derived fatty acids leads to increased cardiac glucose metabolism and heart dysfunction. 2006. *J Biol Chem. 281:8716-8723.*
2. Durgan DJ, Smith JK, Hotze MA, Egbejimi O, Cuthbert KD, Zaha VG, Dyck JR, **Abel ED**, Young ME. Distinct Transcriptional Regulation of Long-Chain Acyl-CoA Synthetase Isoforms and Cytosolic Thioesterase 1 in the Rodent Heart by Fatty Acids and Insulin. 2006. *Am J Physiol Heart Circ Physiol.* 290:H2480-2497.
3. Buerger A, Rozhitskaya O, Sherwood MC, Dorfman AL, Bisping E, **Abel ED**, Pu W, Izumo S, Jay, P.Y. Dilated cardiomyopathy resulting from high-level myocardial expression of Cre-recombinase. 2006.*J. Cardiac Failure. J. Cardiac Failure.* 12:392-398.
4. Lelliot CJ, Medina-Gomez G, Petrovic N, Kis A, Feldmann HM, Bjursell M, Parker N, Curtis K, Campbell M, Hu P, Zhang D, Litwin SE, Zaha VG, Fountain KT, Boudina S, Jimenez-Linan M, Bloun M, Lopez M, Meirhaeghe A, Bohlooly M, Storlien L, Strömstedt M, Snaith M, Ore M, **Abel ED**, Cannon B, Vidal-Puig A. Ablation of PGC-1beta results in defective mitochondrial activity, thermogenesis, hepatic function and cardiac performance. 2006. *PLoS Biology. 4(11):e369.*
5. Sano M, Izumi Y, Helenius K, Asakura M, Rossi DJ, Xie M, Taffet G, Hu L, Pautler RG, Wilson CR, Boudina S, **Abel ED,** Taegtmeyer H, Scaglia F, Graham BH, Kralli A, Shimizu N, Tanaka H, Makela TP, Schneider MD. Menage-a-trois 1 is critical for the transcriptional function of PPARgamma coactivator 1. *Cell Metabolism.* 2007: 5:129-142.
6. Boudina S, Sena S, Theobald H, Sheng X, Wright JJ, Hu XX, Aziz S, Johnson JI, Bugger H, Zaha VG, **Abel ED**. Mitochondrial energetics in the heart in obesity related diabetes: Direct evidence for increased uncoupled respiration and activation of uncoupling proteins. 2007.*Diabetes (In press).*

Reviews

1. Boudina S, **Abel ED**. Mitochondrial uncoupling: a key contributor to reduced cardiac efficiency in diabetes. *Physiology*. 2006:21; 250-258.

2. Hsueh WA, **Abel ED,** Breslow JL, Maeda N, Davis RC, Fisher EA, Dansky H, McClain DA, McIndoe R, Wassef MK, Rabadan-Diehl C, Goldberg IJ. Recipes for creating animal models of diabetic cardiovascular disease. *Circulation Research.* 2007:100; 1415-1427

3. Boudina S, **Abel ED**. Diabetic cardiomyopathy revisited. *Circulation*. 2007: 115; *3213-3223*.